Study of Hydraulic Disturbances From Single-Unit Load Rejection in a Pumped-Storage Hydropower Station With a Shared Water Delivery System

DAQING ZHOU[1], YANAN CHEN[2], HUIXIANG CHEN[3], SHIFAN CHEN[4,5], AND CHUNXIA YANG[1]

[1]College of Energy and Electrical Engineering, Hohai University, Nanjing 210098, China
[2]College of Water Conservancy and Hydropower Engineering, Hohai University, Nanjing 210098, China
[3]College of Agricultural Engineering, Hohai University, Nanjing 210098, China
[4]Chongqing Jiangjin Shipbuilding Industry Company Ltd., Chongqing 402263, China
[5]National Engineering Laboratory for Marine and Ocean Engineering Power System, Shanghai 201108, China

Corresponding authors: Daqing Zhou (zhoudaqing@hhu.edu.cn) and Huixiang Chen (chenhuixiang@hhu.edu.cn)

ABSTRACT The transient characteristics of load rejection process in pumped-storage hydropower (PSH) stations have a close relation to the safety of electric power system and hydraulic facilities. A large portion of PSHs consist of multiple units sharing one tunnel (MUSOT). In this paper, a three-dimensional numerical simulation method for hydraulic disturbance caused by single unit load rejection transition process based on the volume of fluid (VOF) two phase flow model was proposed and a filed test was carried out in a PSH station with a two units sharing one tunnel (TUSOT) setting. The power output from the unit that operates in normal condition (UNC), the pressure fluctuations of the spiral casing inlet and tailrace tunnel outlet, the water level variation and flow pattern in surge tank were obtained through the numerical simulation and field test. The results showed that the highest and lowest water level in surge tank from the numerical method agreed well with the measured data obtained in the field test. The guide vanes closing law of the unit that runs in load rejection (ULR) mainly impacts on the variation of the above parameters. To reduce the influence of single-load load-rejection hydraulic disturbance, a more elaborate guide vanes adjustment scheme of the UNC should be proposed in the next step to avoid large short-time fluctuations in the power output and pressure.

INDEX TERMS Hydraulic disturbances, pumped-storage hydropower, load rejection, shared water delivery system.

I. INTRODUCTION

Pumped-storage hydropower (PSH) stations offer special functions, such as peak shaving, frequency modulation, phase modulation, emergency standby, and black starts. Their advantages of startup and shutdown flexibility and their rapid response capabilities ensure the flexibility and safety of the hydropower system and play an indispensable role in ultra-high voltage and smart grids [1]. For cost and technical reasons, most PSH stations share a water diversion tunnel and water tailrace tunnel, which is referred to as multiple units sharing one tunnel (MUSOT). They utilize a flexible

The associate editor coordinating the review of this manuscript and approving it for publication was Xiaorong Xie.

transmission line scheme such that when some units start up or shut down, no power disturbance occurs among the units [2], [3]. However, for MUSOT, a hydraulic connection exists between the hydraulic units, leading to hydraulic disturbance problems [4]. A hydraulic disturbance is a unique transition process. In the presence of hydraulic connections between units, if some of the units are in full load-rejection operation or the load is drastically increased or decreased, the pressure of the water diversion and tailrace water systems or the water level of the surge tank will fluctuate, affecting the head, flow, and load of units that operate in normal condition (UNC), and ultimately, the hydropower generators and power grids [5]. Therefore, it is of great practical significance to study the dynamic quality and stability of UNC

with hydraulic disturbances to achieve the safe and stable operation of MUSOT hydropower stations and maximize the economic benefits [6].

There have been a number of studies on the hydraulic disturbance problem of hydropower stations. Hannett *et al.* [7] established an equation of state for a hydraulic coupling model of MUSOT hydropower stations, performed simulations with the model, analyzed the hydraulic disturbance process, and verified the model with test results of an actual hydropower station. Chen *et al.* [8] created a computational simulation program to study the hydraulic disturbance problem of a high-head pumped-storage hydropower station in China and simulated the effects on the UNC using the guide vane closing time of the shutdown turbines and the number of the shutdown turbines in the same hydraulic unit. Terrier *et al.* [9] used physical models to study surge wave propagation caused by the combined operations of two pump turbines sharing a common tailrace channel and intake. They measured the flow characteristics associated with the two unit settings and compared them with the prototype test results. They also optimized the equipment operating conditions, and explained the operational limitations. Using the governing equations for surge tanks, Chen *et al.* [10] derived an equation for theoretically calculating the characteristics of the dangerous time interval points of successive load rejections and calculated the surge wave superposition in the successive load rejection of the water delivery system in a hydropower station. Yu *et al.* [11] established a hydraulic transient numerical model of PSH stations for two units sharing one tunnel (TUSOT) based on a transient mathematical model of differential surge tanks with pressure-relief orifices and overflow weirs as well as the actual data of a hydropower station. They performed numerical simulations for the probable transient processes using the model. Xu *et al.* [12] proposed a Hamiltonian mathematical model for multi-hydro-turbine governing systems sharing a common penstock under the excitation of stochastic and shock loads and studied the dynamic characteristics of the systems. Their results showed that the Hamiltonian function could accurately describe the energy variation of hydro-turbine systems in the transient and stable operation. Rezghi and Riasi [13], [14] performed a numerical study on the characteristics of hydraulic transients on two pump-turbine units. The simultaneous emergency shutdown of two turbines, single-turbine load rejection, and two units simultaneously at runaway were investigated. Hou *et al.* [5] performed multi-objective optimization on the successive start-up process in a PSH station in a TUSOT setting. They analyzed the influence of the start-up time steps of the two units and proposed multi-objective optimization scheme with different parameters. Yu *et al.* [15] established a mathematical model of a TUSOT hydraulic system and simulated the transient process caused by the partial load rejection during actual operation of a hydropower station. Furthermore, they proposed theoretical equations for the

power output variation as the pump turbines were subjected to hydraulic disturbances.

The above studies were based on the one-dimensional linear method of characteristics and tests of the transition process. The one-dimensional linear method of characteristics is the most commonly used numerical method for determining hydraulic transients in pipeline systems. However, the boundary conditions are often dependent on the full hydro-mechanical static characteristic curve, and they cannot capture many of the nonlinear pulsating characteristics or the detailed internal flows in the transition process [16], [17]. In addition, the results [18] from tests on the hydraulic disturbance-related transition process showed that the pressure, flow, and power of the UNC were stable to hydraulic disturbances and rapidly converged with time. However, the hydraulic disturbance created a water flow pattern in the diversion tunnel and caused the dynamic quality of the UNC to deteriorate. Although the data obtained by field test methods are accurate and reliable, the costs associated with these tests are high, the internal flow characteristics are difficult to obtain, and the tests on the transition processes pose high risks for safety [19], [20]. Recently, to capture the transient flow pattern during the transition process more accurately, studies on the three-dimensional transition process have received increased attention, due to rapid developments in high-performance computer technology and in computational fluid dynamics [21]–[24]. The previous studies involving three-dimensional calculations mainly examined changes in the hydraulic characteristics during a single-turbine transition [23], [25], [26]. They have not sufficiently dealt with the problem of hydraulic disturbances.

In this study, hydraulic disturbance field tests of single-turbine load rejection in a TUSOT PSH station were first performed. Through using flow rate change to replace the guide blade closing process, a three-dimensional numerical simulation method was developed for the single-turbine load rejection hydraulic disturbance transition process based on the volume of fluid (VOF) two-phase flow model. The power outputs from the UNC, the pressure at the inlet of the spiral casing, the pressure at the outlet of the tailrace tunnel, the fluctuation of the water level, and the water flow pattern of in the surge tank in the water diversion system of the PSH station were studied in terms of hydraulic disturbances to the UNC during load rejection with two different methods of guide vane control. The objective was to establish a new numerical calculation method to study the stability of the entire PSH station system.

II. RESEARCH METHODS
A. THREE-DIMENSIONAL NUMERICAL SIMULATION METHOD
1) RESEARCH OBJECT
A PSH station with TUSOT and tailrace tunnel was studied. The impact of one unit running in load rejection

on another unit running in normal conditions (UNC) and on a hydropower station diversion system was examined. To reduce the degree of difficulty of the numerical simulations, only a model for the pump-turbine system of the UNC was considered for the simulations, and the unit that ran in load rejection (ULR) was simplified using the expected flow variations at the spiral casing inlet and the draft tube outlet.
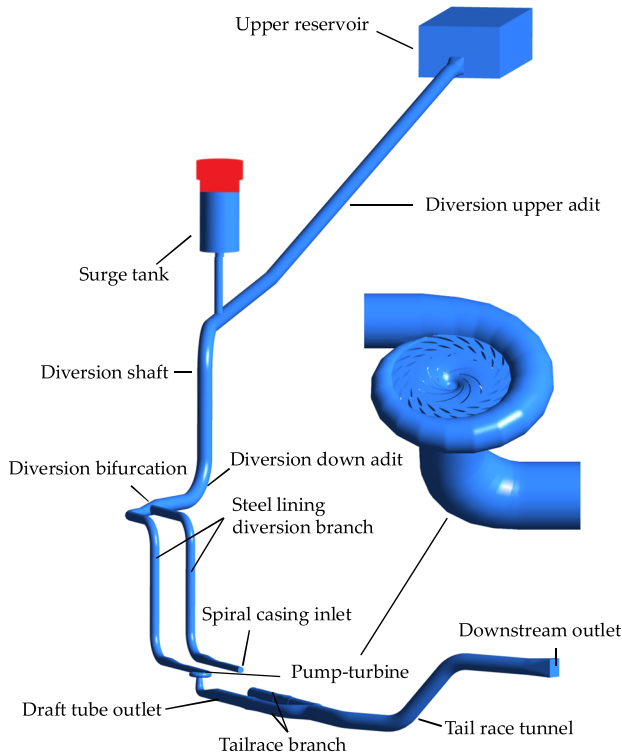

FIGURE 1. Three-dimensional model of a PSH station.

Figure 1 shows a schematic diagram of the structure of the water delivery system of the hydropower station. The water diversion system is 1425–1500 m long and consisted of an inlet/outlet of an upper reservoir, a diversion upper adit, a surge tank, a diversion shaft, a diversion lower adit, a diversion bifurcation, steel lining diversion branches, a ball valve, pump-turbine units, and a tailrace tunnel. The diameters of the water diversion tunnel, branch tunnel, high-pressure pipeline, and tailrace tunnel are 9.00 m, 5.60 m, 7.40 m, and 10.00 m respectively. The hydropower station has a total of four pump turbine units, model HL-LJ-550. The main parameters of the pump turbine are as follows: the moment of inertia of the unit is 193002 t·m², the rated output of the turbine is 306 MW, the rated speed is 250 rpm, the rated flow rate is 176.1 m³/s, and the rated head is 195 m. The regions in the calculation include the diversion upper tunnel, surge tank, diversion bifurcation, pump turbines, and diversion lower tunnel.

2) GOVERNING EQUATIONS
In the calculation of the hydraulic disturbance transition process of the hydropower station model, to make the calculation

more consistent with the actual physical conditions and achieve faster convergence, we used a steady calculation to first determine the flow field before a disturbance was introduced, after which we used an unsteady calculation to model the transient process. In the steady calculation, a single-phase flow model was used, while in the unsteady calculations, a VOF model was used.

In the VOF model [21], [27], for the water and gas two-phase flow, F was the volume ratio of water in each control unit, and the volume ratio of the gas in the control unit was $1 - F$. The density and dynamic viscosity were calculated as follows:

$$\rho = F\rho_1 + (1 - F)\rho_2 \tag{1}$$
$$\mu = F\mu_1 + (1 - F)\mu_2 \tag{2}$$

where ρ_1 and ρ_2 are the densities of the liquid and gas phase, respectively, and μ_1 and μ_2 are the dynamic viscosities of the liquid and gas phase, respectively.

The fundamental governing equations based on the VOF two-phase flow model were as follows [28]:

Continuity equation:

$$\frac{\partial \rho}{\partial t} + \nabla \cdot (\rho \boldsymbol{u}) = 0 \tag{3}$$

Momentum conservation equation:

$$\frac{\partial \rho \boldsymbol{u}}{\partial t} + (\rho \boldsymbol{u} \cdot \nabla) \boldsymbol{u} = -\nabla p + (\mu + \mu_t) \nabla^2 \boldsymbol{u} + \boldsymbol{S}_M \tag{4}$$

In these equations, symbols ρ, $\boldsymbol{u}$, t, p, μ *and* μ_t stand for the average density of the volume fraction, velocity, time, pressure, dynamic viscosity coefficient, and the turbulent viscosity respectively. $\mu_t = \rho C_\mu k^2 / \varepsilon$, where C_μ is a constant, symbols ∇, ∇^2 and $\boldsymbol{S}_M$ stands for the Hamilton operator, Laplacian operator and is source term respectively.

In the continuity and motion equations of the two-phase flow, the single-phase flow equation density was constant, so all items in the single-phase flow equation could be divided by the density. The used turbulence model was a standard k-ε model based on the VOF two-phase flow model [29], [30].

3) MESH GENERATION AND CALCULATION METHODS
ANSYS ICEM was used to generate meshes in the regions of the computational domain and verify the mesh independence. The final total number of grid cells was determined to be 6.85 million, as shown in Figure 2. Table 1 shows the grid details for each part after the model mesh was determined.

The calculations were divided into the steady and unsteady calculations. First, the steady calculation was performed for the flow field, and the finite volume method was used to solve the governing equations discretely [31], [32]. The central difference scheme was used for the pressure term. The first-order upwind difference scheme was used for the velocity term, the turbulent kinetic energy term, and the turbulent viscous coefficient term. The velocity-pressure coupling equation was solved based on the SIMPLEC algorithm. The VOF multiphase flow model was subsequently used for the
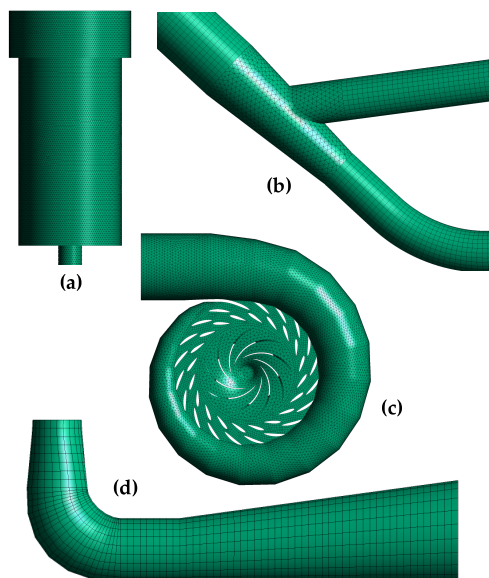
FIGURE 2. Mesh grids of the model at different locations: (a) surge tank, (b) diversion bifurcation, (c) pump-turbine, and (d) tailrace tunnel.

TABLE 1. Type and number of mesh elements in different locations.

Location	Mesh type	Number (million)
Diversion Upper Adit	Hexahedral	1.01
Surge Tank	Hexahedral	1.48
Diversion Bifurcation	Tetrahedral	0.35
Turbine	Tetrahedral /Hexahedral	3.40
Downstream Tunnel	Hexahedral	0.61
Total		6.85

unsteady calculation. The water was the main phase, and the gas was the secondary phase. Furthermore, based on the discretized finite volume method governing equations, PRESTO was used for the pressure term, while the first-order upwind difference scheme was chosen for the velocity, turbulent kinetic energy, and turbulent viscosity coefficient terms. The velocity–pressure coupling equation was solved using the PISO algorithm [33], with the effects of gravity taken into account.

4) BOUNDARY CONDITIONS AND CALCULATION CONDITIONS

(a) Definition of inlet and outlet boundary: A suitably sized reservoir was added to the inlet of the water leveling tunnel. The ''pressure inlet'' boundary condition (49050 Pa) was set at the upper reservoir's water surface, while the ''pressure outlet'' boundary condition was imposed at the downstream outlet surface. The outlet pressure distribution was obtained based on the submerged depth of the downstream reservoir.

(b) Definition of load rejection boundary: The process of load rejection was the closing process of the guide vane. It resulted in a continual decrease in the flow rate with time in the tunnel. Therefore, the numerical calculation was simplified in the simulation of the load rejection process of the

unit by a flow rate variation, which was added as a boundary condition to the spiral casing inlet of the load rejection unit using the UDF program. Meanwhile, the adjustment of UNC guide vanes was not considered in the numerical simulations. To simultaneously study the influence of the hydraulic disturbance on the downstream tunnels, the same flow rate variation process was also set up at the outlet of the load rejection unit.

(c) Definition of the outlet boundary of the surge tank: In the steady calculation, the outlet boundary of the surge tank was defined as the WALL boundary, and the initial height of the water level in the surge tank was calculated to allow for rapid convergence. The pressure outlet boundary condition was used in the unsteady calculation, and the state was defined as a gas by the VOF two-phase flow model, in which the gas was freely flowing in and out of the outlet surface of the surge tank throughout the calculation process.

It was determined from the experimental data that the flow reduction time of the load-rejection unit was 32.5 s. Because the unit operated in a large-scale power grid, its running speed was constant at 250 rpm, and the calculation time was 180 s. To ensure the accuracy of the calculation, after trials and time-step-independence verification, the calculation time step was determined to be 0.001 s.

B. TEST METHODS

In the field tests of the hydraulic disturbance in the pumped-storage station, once the state parameters of the unit met the test requirements, the test measurement system issued load rejection instructions to the load rejection unit through the monitoring system of the power plant. Then, the load rejection unit circuit breaker was disconnected, and the governor closed the guide vanes according to the ULR curve in the figure 3. The guide vane closing time of the ULR was $t_2 = 32.5$ s and the closing angle was 34.6°. Meanwhile, the guide vanes of the UNC were closed at a small angle of 4.8° at time $t_1 = 14.3$ s (Figure 3). At the same time, the test measurement system collected the stator current signal from the generator in normal operation through the monitoring system of the power plant. Since the unit was connected to a large power grid, the voltage remained unchanged, and changes in the output power of the normal operation unit came from changes in the current. In addition, pressure variations at the inlet (elevation: 46.13 m) of the spiral casing and the outlet (elevation: 37.63 m) of the draft tube were measured by the KELLER pressure transducer. The water level fluctuation of the surge tank was monitored by STS liquid level transmitter. The whole test measurement system guaranteed the consistency of signal acquisition time through synchronizer.

III. RESULTS AND ANALYSIS
A. FLUCTUATION OF POWER OUTPUT OF THE UNC
Based on the analysis of the hydraulic disturbances during the normal operation of the large power grid, the power output fluctuation of the UNC under the influence of the load-rejection unit is an important indicator to evaluate the
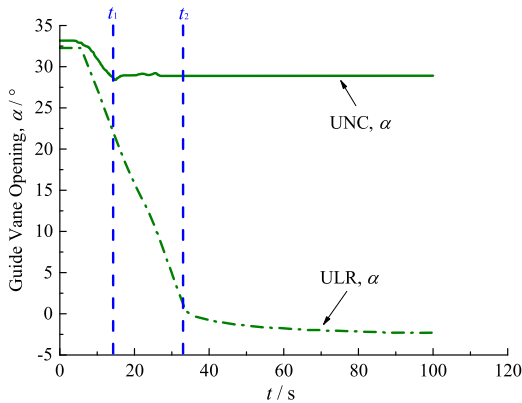
FIGURE 3. Guide vane adjustment schemes of the two units in the field test of single-unit load rejection of the TUSOT system.
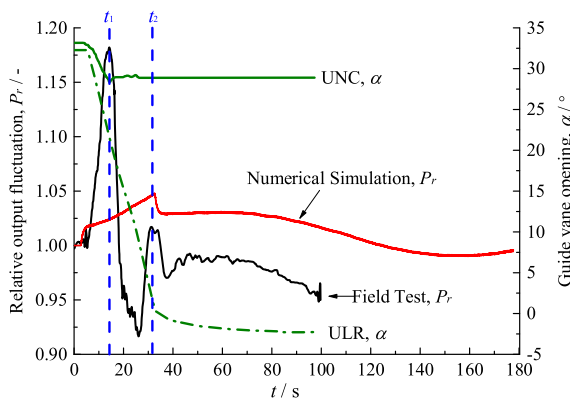

FIGURE 4. Relative fluctuation of power output of the UNC during single-unit load rejection from the hydropower station with the TUSOT system.

impact of the hydraulic disturbance transition process on the power grid system. Figure 4 shows the relative power output fluctuation of the UNC under the single-turbine load-rejection mode for the TUSOT operational setting. The red curve represents the power output fluctuation value obtained by the numerical simulation. The black curve represents the power output variation curve obtained by the hydropower station field tests. The green curves represent the regulation scheme of the guide vanes of the unit during the field tests.

During the guide vanes closing process of the load-rejection unit ULR, the guide vanes of the UNC were closed at a low speed as well. Due to the closing of the guide vane, the upstream tunnels generated a positive water hammer, increasing the pressure and causing more water to flow into the UNC, resulting in a sudden power output increase in the in the same unit. At $t = t_1$, the power output increased to the first peak (1.18 times the initial value), corresponding to a complete closure of UNC guide vanes. This closing way led to a peak value of the P_r curve at t_1. Starting from time t_1, the power output of the UNC suddenly dropped. This was due to the lag in the reduction effect of the closing of the guide vane of the UNC on the flow rate. The power output was rapidly reduced to 0.91 times of the initial value.

However, because the numerical calculation method did not simulate the guide vane closing process of the UNC, the power output continued to rise without fluctuation. Since the flow rate of the load-rejection unit continued to decrease, the positive water hammer generated in the upstream tunnel system caused the curve of the UNC to reach a second peak at t_2 of 1.02 times the initial value. t_2 was the turning point at which the closing of the guide vane of the ULR had basically completed. The peak of the power output obtained by the numerical simulation also reached its maximum value (1.04 times the initial value) at this moment, which was higher than the measured value. After the guide vane of the UNC was closed, the power output curves of the numerical simulation and the field tests first dropped sharply and subsequently slowly decreased with some oscillations. The comparison of the data from the numerical simulation and the field tests showed that the occurrence time of the power output extreme values under single-unit load rejection was greatly affected by the guide vanes closing, and the data of both methods showed that the extreme values were reached at the same time. The field test results showed that when participating in the adjustment, the guide vanes of the UNC caused the power output to fluctuate drastically with larger amplitude for a short period of time. The numerical simulation results showed that the inaction of the adjustment mechanism of the UNC during the single-unit load rejection process could effectively alleviate the large fluctuations of the power output, but it took longer for the power output to return to the initial value.

B. PRESSURE FLUCTUATION OF THE UNC AT UPSTREAM AND DOWNSTREAM MEASURING POINTS

Figure 5 shows the relative fluctuation of the pressure at upstream and downstream points of the UNC in the TUSOT hydropower station. As shown in Figure 5a, the inlet pressure of the spiral casing of the UNC continually rose during the load rejection process of the ULR. In the early stage of load rejection, the pressure increased more rapidly, and the subsequent rise was slower until the guide vanes closing process of the ULR basically completed at time t_2, at which time the pressure reached a maximum value at approximately 1.04 times the initial pressure. After the ULR load rejection process ended, the pressure of the spiral casing of the UNC dropped sharply to 1.025 times the initial pressure. After that, the pressure gradually increased back until 70 s, and subsequently began to drop to 0.99 times of the initial pressure ($t = 152$ s). From the field test results, during the ULR load rejection process, the pressure at the spiral casing inlet of the UNC suddenly increased to its first peak at t_1, before dropping back to lower values. This took source from the guide vanes adjustment within the UNC. The following peak was reached at t_2, which is found to be associated to the hydraulic disturbances from the ULR load rejection process. Both the field test and numerical simulation methods showed pressure surges at t_2, after which stability got restored for a period of time, before gradually decreasing to lower values.
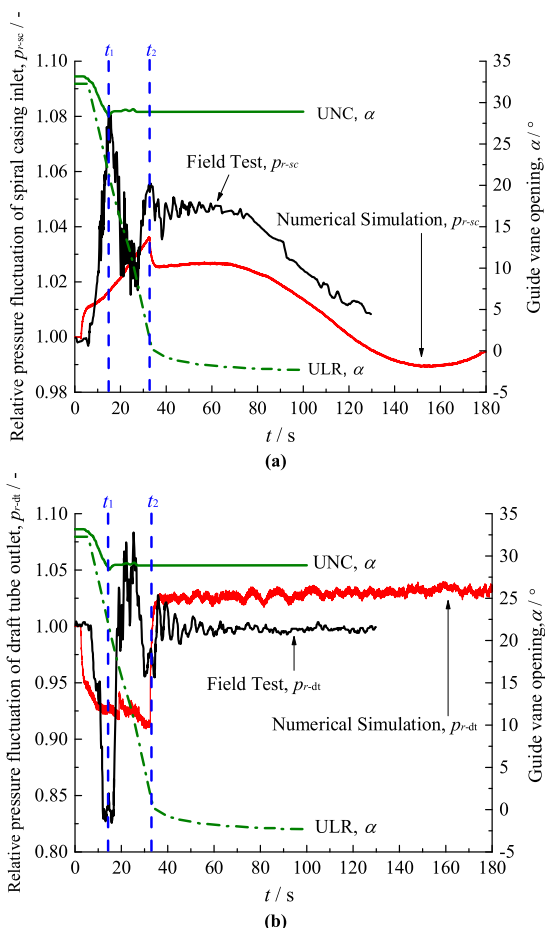
FIGURE 5. Relative fluctuation of pressure of the UNC during single-unit load rejection from the hydropower station with the TUSOT system: (a) spiral casing inlet and (b) tailrace outlet.

FIGURE 6. Variation curve and test data of the water level of the surge tank in the water diversion system during single-unit load rejection from the hydropower station with the TUSOT system.

Comparing the change of the pressure at the inlet of the spiral casing and the change of the power output of the UNC, the change of the pressure of the spiral casing was consistent with the variation of the power output in both the field test data and the numerical simulation data.

The numerical simulation curve in Figure 5b shows that when the ULR began to reject the load, the pressure at the outlet of the tailrace tunnel of the UNC dropped sharply and subsequently gradually decreased, which was caused by the negative water hammer of the downstream pipeline of the ULR unit. When the guide vanes of the ULR were closed at t_2, due to the impact of the positive water hammer, the pressure at the outlet of the tailrace tunnel of the UNC rose instantaneously and fluctuated with a small amplitude around 1.025 times the initial value. The field test showed that, similar to the change of the spiral casing inlet pressure and power output, due to the dual influence of the different guide vanes adjustment schemes of the two units, the outlet pressure of the tailrace tunnel suddenly increased at t_2 after undergoing a similar cycle of variations, after which it fluctuated until 80 s and remained basically stable.

The field test curve of the pressure change of the UNC at the upstream and downstream measuring points indicated that
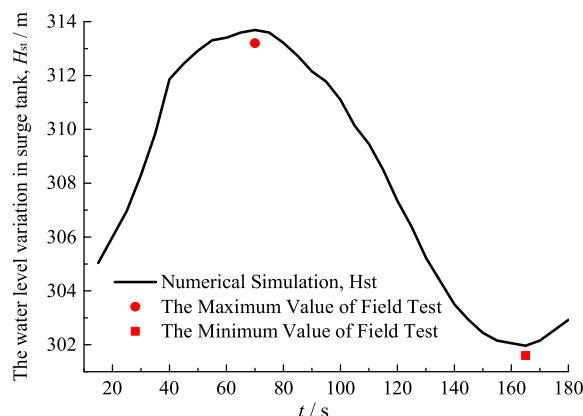
the pressures of the spiral casing inlet and the outlet of the tailrace tunnel abruptly changed at the end of the small-angle closing of the guide vane of the UNC. The numerical simulation was not influenced by the closing of the guide vanes of the UNC, so the pressure continued to change without fluctuations. Meanwhile, the field test pressure abruptly changed again at the end of the guide vanes closing of the ULR, and its extremes occurred at the same time in the numerical simulation and the field test. Comparing the two adjustment schemes in the field test and in the numerical simulation, it was evident that during the single-unit load-rejection process, the pressure change and power output change of the UNC were caused by the action of the water guide mechanism. To reduce the large-amplitude fluctuations of the pressure and the power output during the initial load rejection of the ULR, it was necessary to explore a more appropriate guide vanes adjustment scheme for the UNC.

C. FLUCTUATIONS OF WATER LEVEL AND WATER FLOW PATTERN IN THE SURGE TANK OF THE WATER DIVERSION SYSTEM

Figure 6 shows the maximum and minimum values of the water level in the surge tank obtained from the numerical simulation and the field test when one turbine was operating under normal conditions and the other turbine was in load rejection mode in the TUSOT conditions. The figure shows the change of water level when the water body in the surge tank was affected by the single-load rejection process, namely, a rising-falling-rising fluctuation process. The highest water levels of 313.69 and 313.20 m were obtained by the numerical simulation and the field test, respectively. The value obtained by the field test was 0.49 m higher. The lowest water levels of 301.96 and 301.60 m were obtained by the numerical simulation and the field test, respectively. The value obtained by the field test was 0.36 m higher. The water levels reached extreme values at the same time in the numerical simulation and the field test.
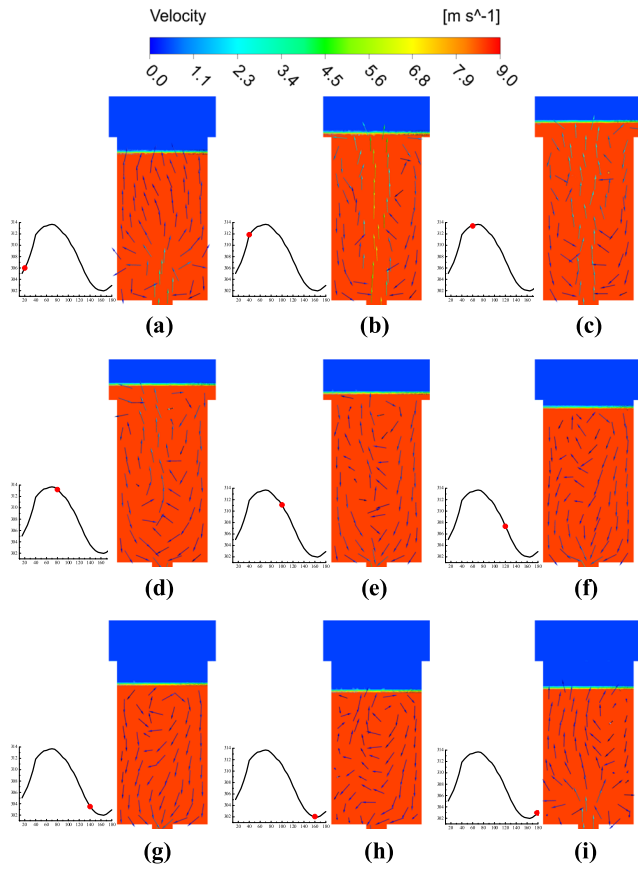
FIGURE 7. Water level fluctuation and flow pattern of the surge tank in the water diversion system during single-unit load rejection in the hydropower station with the TUSOT system: (a) t=20 s, (b) t=40 s, (c) t=60 s, (d) t=80 s, (e) t=100 s, (f) t=120 s, (g) t=140 s, (h) t=160 s, and (i) t=180 s.

Figure 7 shows the changes of the water level and flow velocity in the surge tank. In the figure, a, b, c, d, e, f, g, h, and i are the water levels of the surge tank at 20, 40, 60, 80, 100, 120, 140, 160, and 180 s of the calculation, respectively. The red and blue areas in the figure represent the water and gas body. The arrows represent the water flow velocity, and the intermediate transition color represents the gas–liquid interface regions.

The analysis of the flow patterns in the surge tank showed that at the initial moment of the water level rise (Figure 7(a)), a large amount of water was poured into the surge tank from the impedance orifice, and backflow formed at the bottom plate of the surge tank and created vortices. Subsequently (Figure 7(b)), the orifice overcurrent flow rate increased, and the area of vortices expanded and began to move up. When the water level was close to the highest water level (Figure 7(c)), the flow velocity at the impedance orifice decreased rapidly, and the water flow pattern in the surge tank began to become turbulent. When the water level began to decrease (Figure 7(d)), the water in the surge tank flowed downward along the side wall of the surge tank and subsequently surged toward the impedance orifice when approaching the bottom

plate of the surge tank. At this point, the water flow pattern in the middle of the surge tank was very turbulent. During the water level lowering process (Figure 7(e), (f), and (g)), the flow direction of the surge tank still pointed downward along the side wall but was random the middle. When the water level in the surge tank was near the lowest value (Figure 7(h)), the water flow velocities were approximately zero, and the water flow pattern was random with no evident patterns. However, when the water level rose again (Figure 7(i)), the water flow in the impedance orifice began to flow upward again, and the flow pattern was similar to that of the initial rise, but with a reduced flow rate.

IV. CONCLUSION

A VOF two-phase flow model and field test were used to study the single-turbine load rejection hydraulic disturbance problem in different guide vanes adjustment schemes in a PSH station with a TUSOT setting. The fluctuations of the power output, the pressure of the spiral casing inlet, the pressure of the tailrace tunnel outlet, and the water level in the surge tank were analyzed. The highest and lowest water level of the surge tank from the analysis agreed well with the measured data as obtained from the field tests.

When the single-turbine load rejection transition process occurred, if the guide vanes action of the UNC operated normally, the unit power output, the spiral casing inlet pressure, and the tailrace outlet pressure exhibited large short-term fluctuations. If the guide vane of the UNC did not operate, the fluctuations of the above parameters were mainly affected by the adjustment scheme of the guide vane closing of the ULR. In addition, the water hammer formed at the end of the closing of the guide vane caused the power output of the UNC to peak. When the adjustment of the water diversion mechanism was completed, the power output and pressure entered a steady fluctuation process. Therefore, to reduce the influence of single-load load-rejection hydraulic disturbance, the water diversion mechanism of the UNC during load rejection must use a more elaborate adjustment scheme to avoid large short-time fluctuations in the power output and pressure. During the load-rejection transition process, the water level in the surge tank first increased and subsequently decreased. While the water level increased, the outflow from the impedance orifice caused backflow at the side wall, and vortices formed. When the water level decreased, the water did not all flow to the orifice, and the flow directions of the water in the central part of the surge tank were random.

In the next step, complete modeling of the load rejection unit with the inclusion of the guide vanes adjustment process of the UNC was carried out to more realistically simulate the hydraulic disturbance problem during the single load rejection process, to reduce the calculation error caused by the simplification in the boundary conditions and to be verifiable by the comparison with measured data. In addition, for a PSH station with the TUSOT setting, numerical simulations should be carried out to explore the hydraulic disturbance problems

during the transition such as successive load rejections and successive single-turbine load increases.

REFERENCES

[1] A. Harby, J. Sauterleute, M. Korpas, A. Killingtveit, E. Solvang, and T. Nielsen, "Pumped storage hydropower," in *Transition to Renewable Energy Systems*. Hoboken, NJ, USA: Wiley, 2013, pp. 597–618.

[2] S. Rehman, L. M. Al-Hadhrami, and M. M. Alam, "Pumped hydro energy storage system: A technological review," *Renew. Sustain. Energy Rev.*, vol. 44, pp. 586–598, Apr. 2015. doi: 10.1016/j.rser.2014.12.040.

[3] J. I. Pérez-Díaz, M. Chazarra, J. García-González, G. Cavazzini, and A. Stoppato, "Trends and challenges in the operation of pumped-storage hydropower plants," *Renew. Sustain. Energy Rev.*, vol. 44, pp. 767–784, Apr. 2015. doi: 10.1016/j.rser.2015.01.029.

[4] D. Zhou, H. Chen, and S. Chen, "Research on hydraulic characteristics in diversion pipelines under a load rejection process of a PSH station," *Water*, vol. 11, no. 1, p. 13, Jan. 2019. doi: 10.3390/w11010044.

[5] J. Hou, C. Li, W. Guo, and W. Fu, "Optimal successive start-up strategy of two hydraulic coupling pumped storage units based on multi-objective control," *Int. J. Elect. Power Energy Syst.*, vol. 111, pp. 398–410, Oct. 2019. doi: 10.1016/j.ijepes.2019.04.033.

[6] S. Mansoor, "Modelling of a pump-storage units supplied from a common tunnel," in *Proc. ICCAAI*. Lancaster, U.K.: Destech Publicat, 2015, pp. 37–42.

[7] L. N. Hannett, J. W. Feltes, B. Fardanesh, and W. Crean, "Modeling and control tuning of a hydro station with units sharing a common penstock section," *IEEE Trans. Power Syst.*, vol. 14, no. 4, pp. 1407–1414, Nov. 1999. doi: 10.1109/59.801904.

[8] N. Chen, Y. Zhang, Q. Tu, and Z. Met, "Study on transients and it's stability in pumped storage power station under hydraulic turbulence," *J. Hydraul. Eng.*, vol. 10, pp. 68–74, Oct. 1996.

[9] S. Terrier, M. Bieri, G. De Cesare, and A. J. Schleiss, "Surge wave propagation in a common tailrace channel for two large pumped-storage plants," *J. Hydraul. Eng.*, vol. 140, pp. 218–225, Feb. 2014. doi: 10.1061/(asce)hy.1943-7900.0000809.

[10] S. Chen, J. Zhang, and X. Yu, "Surge superposition following successive load rejection in hydropower stations," *J. Hydraul. Eng.*, vol. 46, pp. 1321–1328, Nov. 2015. doi: 10.13243/j.cnki.slxb.20150121.

[11] X. Yu, J. Zhang, and L. Zhou, "Hydraulic transients in the long diversion-type hydropower station with a complex differential surge tank," *Sci. World J.*, vol. 2014, Jul. 2014, Art. no. 241868. doi: 10.1155/2014/241868.

[12] B. Xu, F. Wang, D. Chen, and H. Zhang, "Hamiltonian modeling of multi-hydro-turbine governing systems with sharing common penstock and dynamic analyses under shock load," *Energy Convers. Manage.*, vol. 108, pp. 478–487, Jan. 2016. doi: 10.1016/j.enconman.2015.11.032.

[13] A. Rezghi and A. Riasi, "The interaction effect of hydraulic transient conditions of two parallel pump-turbine units in a pumped-storage power plant with considering 'S-shaped' instability region: Numerical simulation," *Renew. Energy*, vol. 118, pp. 896–908, Apr. 2018. doi: 10.1016/j.renene.2017.11.067.

[14] A. Rezghi and A. Riasi, "Sensitivity analysis of transient flow of two parallel pump-turbines operating at runaway," *Renew. Energy*, vol. 86, pp. 611–622, Feb. 2016. doi: 10.1016/j.renene.2015.08.059.

[15] X. D. Yu, Q. Zhou, L. Zhang, and J. Zhang, "Hydraulic disturbance in multiturbine hydraulically coupled systems of hydropower plants caused by load variation," *J. Hydraul. Eng.*, vol. 145, no. 1, Jan. 2019. doi: 10.1061/(asce)hy.1943-7900.0001548.

[16] J. Zhou, Y. Xu, Y. Zheng, and Y. Zhang, "Optimization of guide vane closing schemes of pumped storage hydro unit using an enhanced multi-objective gravitational search algorithm," *Energies*, vol. 10, no. 7, p. 911, Jul. 2017. doi: 10.3390/en10070911.

[17] Z. Li, H. Bi, B. Karney, Z. Wang, and Z. Yao, "Three-dimensional transient simulation of a prototype pump-turbine during normal turbine shutdown," *J. Hydraul. Res.*, vol. 55, no. 4, pp. 520–537, 2017. doi: 10.1080/00221686.2016.1276105.

[18] G. D. Li, J. Ding, and X. Yu, "Study of hydraulic disturbance test and predetermination of pumped-storage unit," *Dongfang Electr. Rev.*, vol. 29, no. 1, pp. 37–39, Mar. 2015. doi: 10.13661/j.cnki.issn1001-9006.2015.01.009.

[19] C. Trivedi, M. J. Cervantes, and O. G. Dahlhaug, "Numerical techniques applied to hydraulic turbines: A perspective review," *Appl. Mech. Rev.*, vol. 68, no. 1, Jan. 2016, Art. no. 010802. doi: 10.1115/1.4032681.

[20] C. Trivedi, M. J. Cervantes, B. K. Gandhi, and O. G. Dahlhaug, "Erratum to: Experimental investigations of transient pressure variations in a high head model Francis turbine during start-up and shutdown," *J. Hydrodyn.*, vol. 26, no. 2, pp. 277–290, 2014. doi: 10.1007/s42241-018-0114-6.

[21] D. Zhou, H. Chen, and L. Zhang, "Investigation of pumped storage hydropower power-off transient process using 3D numerical simulation based on SP-VOF hybrid model," *Energies*, vol. 11, no. 4, p. 1020, Apr. 2018. doi: 10.3390/en11041020.

[22] X. Fu, D. Li, H. Wang, G. Zhang, Z. Li, and X. Wei, "Influence of the clearance flow on the load rejection process in a pump-turbine," *Renew. Energy*, vol. 127, pp. 310–321, Nov. 2018. doi: 10.1016/j.renene.2018.04.054.

[23] G. Pavesi, G. Cavazzini, and G. Ardizzon, "Numerical simulation of a pump–turbine transient load following process in pump mode," *J. Fluids Eng.*, vol. 140, no. 2, Feb. 2018, Art. no. 021114. doi: 10.1115/1.4037988.

[24] D. Li, X. Fu, Z. Zuo, H. Wang, Z. Li, S. Liu, and X. Wei, "Investigation methods for analysis of transient phenomena concerning design and operation of hydraulic-machine systems—A review," *Renew. Sustain. Energy Rev.*, vol. 101, pp. 26–46, Mar. 2019. doi: 10.1016/j.rser.2018.10.023.

[25] D. Zhou, H. Chen, J. Zhang, S. Jiang, J. Gui, C. Yang, and A. Yu, "Numerical study on flow characteristics in a francis turbine during load rejection," *Energies*, vol. 12, no. 4, p. 716, Feb. 2019. doi: 10.3390/en12040716.

[26] X. Fu, D. Li, H. Wang, G. Zhang, Z. Li, and X. Wei, "Analysis of transient flow in a pump-turbine during the load rejection process," *J. Mech. Sci. Technol.*, vol. 32, no. 5, pp. 2069–2078, May 2018. doi: 10.1007/s12206-018-0416-1.

[27] M. M. Karim, B. Prasad, and N. Rahman, "Numerical simulation of free surface water wave for the flow around NACA 0015 hydrofoil using the volume of fluid (VOF) method," *Ocean Eng.*, vol. 78, pp. 89–94, Mar. 2014. doi: 10.1016/j.oceaneng.2013.12.013.

[28] X. Tian, Q. Wang, G. Liu, W. Deng, and Z. Gao, "Numerical and experimental studies on a three-dimensional numerical wave tank," *IEEE Access*, vol. 6, pp. 6585–6593, 2018. doi: 10.1109/access.2018.2794064.

[29] B. E. Launder and D. B. Spalding, "The numerical computation of turbulent flows," *Comput. Methods Appl. Mech. Eng.*, vol. 3, pp. 269–289, Mar. 1974. doi: 10.1016/0045-7825(74)90029-2.

[30] F. Wang, *Computational Fluid Dynamics Analysis*. Beijing, China: Tsinghua Univ. Press, 2004.

[31] D. Li, H. Wang, Z. Li, T. K. Nielsen, R. Goyal, X. Wei, and D. Qin, "Transient characteristics during the closure of guide vanes in a pump-turbine in pump mode," *Renew. Energy*, vol. 118, pp. 973–983, Apr. 2018. doi: 10.1016/j.renene.2017.10.088.

[32] K. Kan, Y. Zheng, Y. Chen, Z. Xie, G. Yang, and C. Yang, "Numerical study on the internal flow characteristics of an axial-flow pump under stall conditions," *J. Mech. Sci. Technol.*, vol. 32, no. 10, pp. 4683–4695, Oct. 2018. doi: 10.1007/s12206-018-0916-z.

[33] L. Fu and Y. Wang, "Load shedding test and simulation analysis of hydropower station with surge shaft," *Water Resour. Power*, vol. 30, no. 6, pp. 154–157, Jun. 2012.

DAQING ZHOU received the B.S. degree in water conservancy and hydropower power engineering and the M.S. degree in water conservancy and hydropower engineering from Hohai University, Nanjing, China, in 1998 and 2002, respectively, and the Ph.D. degree in power engineering and engineering thermal physics from Tsinghua University, in 2007. He is currently an Associate Professor with the College of Energy and Electrical Engineering, Hohai University. His research interests include hydraulic transient of hydraulic machinery and systems, and design and performance optimization of fluid machinery.

YANAN CHEN received the B.S. degree in water conservancy and hydropower engineering from China Three Gorges University, in 2018. She is currently pursuing the master's degree in water conservancy and hydropower engineering with Hohai University.

SHIFAN CHEN received the B.S. degree in thermal energy and power engineering from the Northwest A& F University, in 2011, and the M.S. degree in fluid machinery and engineering from Hohai University, in 2014. He is currently with the Chongqing Jiangjin Shipbuilding Industry Company Ltd., Chongqing, China, and the National Engineering Laboratory for Marine and Ocean Engineering Power System, Shanghai, China.

HUIXIANG CHEN received the B.S. degree in thermal energy and power engineering and the Ph.D. degree in water conservancy and hydropower engineering from Hohai University, Nanjing, China, in 2012 and 2019, respectively, where she is currently a Lecturer with the College of Agricultural Engineering. Her research interests include hydraulics of hydropower plant and pump station, hydraulic transient, and safety control of hydraulic units.

CHUNXIA YANG received the B.S. degree in thermal energy and power engineering and the Ph.D. degree in water conservancy and hydropower engineering from Hohai University, Nanjing, China, in 2010 and 2015, respectively, where she is currently a Lecturer with the College of Energy and Electrical Engineering.

• • •